SPIN COATED GALLIUM OXIDE THIN FILMS AND THE EFFECT OF Mo-DOPING CONCENTRATION ON LUMINESCENCE PROPERTIES

WANG TIANKUN

UNIVERSITI SAINS MALAYSIA

2023

SPIN COATED GALLIUM OXIDE THIN FILMS AND THE EFFECT OF Mo-DOPING CONCENTRATION ON LUMINESCENCE PROPERTIES

by

WANG TIANKUN

Thesis submitted in fulfilment of the requirements
for the degree of
Doctor of Philosophy

July 2023

ACKNOWLEDGEMENT

First and foremost, I would like to express my deepest gratitude to my supervisor, Assoc. Prof. Dr. Ng Sha Shiong, for his valuable guidance, detailed support, and patience throughout this research. He has always given me enough freedom to explore my own interests while also giving me enough support to improve my work. Because of the Covid-19 condition, the research work and study life have become more difficult; Dr. Ng also has given me a lot of concern about the study life on campus.

Next, I wish to acknowledge the staff at the Institute of Nano Optoelectronics Research and Technology (INOR) and Nano-Optoelectronics Research & Technology Laboratory (NOR Lab.) of the School of Physics, Universiti Sains Malaysia, for their kind assistance in handling the equipment and characterization systems. I am also grateful to Dr. Lim Wong Foong and both the previous and present secretaries of INOR for giving help in the matters of entering Malaysia during the movement control order (MCO) period. Apart from that, I am very thankful to Maizaitul Akmam Bt Ab Hamid, Tan Aik Kwan, Lau Khai Shenn, Alghareeb Abbas Abdulhussein Mohammed, Deng Junchen, and Suvindraj Rajamanickam. Although some of them work in different research groups and different projects, they always give me the help they can provide.

I am thankful for the financial support from the Ministry of Higher Education Malaysia through the Fundamental Research Grant Scheme (Project Code: FRGS/1/2018/STG07/USM/02/10).

Last but not least, to my family, thank them for supporting me and giving the unconditional love and understanding.

TABLE OF CONTENTS

LIST OF TABLES

Page

LIST OF FIGURES

Page

LIST OF SYMBOLS

A	Constant for direct transition
a, b, c, β	Lattice constants
c	Velocity of light
C_P	Contrast of one PL emission peak
D_c	Crystallite size
d_m	Lattice distance between the (hkl) planes
e	Electron charge
E	Young's modulus
$E\|\|a, E\|\|b, E\|\|c$	Electric field parallel to a, b, c edge
E_C	Conduction band
E_g	Energy band gap
E_V	Valence band
h	Planck constant
$\hbar$	Reduced Planck constant
h,k,l	Miller-Bravais indices
hv	Photon energy
I_I, I_{II}	PL intensity of peaks I and II
k	Wave number
k_B	Boltzmann constant
m_0	Electron mass
m_e^*	Effective electron mass
Rq	Root mean square roughness
$\%R$	Reflectance
S_{ij}	Elastic compliance
u	Energy density

V_{Ga}, V_{Ga}^{x}	Ga vacancy
V_O, V_O^x	O vacancy
V_O-V_{Ga}, $(V_{Ga} - V_O)^x$	O-Ga vacancy pair
w/o	Without
β_D, Δf	Full width at the half-maximum intensity
β_S	Strain induced by broadening
β_t	Total physical line broadening
δ	Dislocation density
ε	Crystal strain
ε_d	Dielectric medium
θ	Bragg's angle
κ	Constant (0.9)
λ	Wavelength
σ_L	Lattice deformation stress
Φ_E	PL spectra based on photon energy
Φ_λ	PL spectra based on wavelength

LIST OF ABBREVIATIONS

AFM	Atomic force microscopy
BZ	Brillouin zone
CVD	Chemical vapor deposition
DFT	Density functional theory
DI water	Deionized water
DUV	Deep ultra-violet
e-h	Electron-hole
ET	Energy transfer
FEM	Finite element method
FESEM	Field-emission scanning electron microscopy
FTIR	Fourier-transform infrared spectroscopy
FWHM	Full width at half-maximum
GID	Grazing incidence diffraction
HDF	Hybrid functional
HT	Heat treatment
HVPE	Halide vapor phase epitaxy
ITB	Incoherent twin boundaries
LED	Light-emitting diode
MBE	Molecular beam epitaxy
MOCVD	Metal-organic chemical vapor deposition
NIR	Near-infrared
PL	Photoluminescence
PLD	Pulsed laser deposition
PreT	Pretreatment
PT	Plasma treatment
RGB	Red, green, and blue
SSP	Size-strain plots
TCO	Transparent conductive oxide
UV	Ultra-violet
UV-Vis	Ultraviolet-visible
W-H	Williamson-hall

XRD	X-ray diffraction

SALUTAN PUTARAN PERTUMBUHAN FILEM NIPIS GALIUM OKSIDA DAN KESAN KEPEKATAN PENGEDOPAN Mo KE ATAS SIFAT LUMINASI

ABSTRAK

Galium oksida jenis beta (β-Ga_2O_3) dengan tenaga jurang jalur lebar ultra dan sifat pancaran yang baik sesuai untuk aplikasi optoelektronik seperti peranti luminasi. Walau bagaimanapun, pertumbuhan filem β-Ga_2O_3 berkualiti baik menggunakan teknik kos rendah dan mudah, terutamanya teknik salutan putaran sol-gel, masih kekal mencabar. Untuk ciri luminasi, kedua-dua β-Ga_2O_3 yang tidak didop dan didop memancarkan pancaran pelbagai warna disebabkan oleh paras pelbagai tenaga bagi kekosongan intrinsik, yang tidak baik untuk aplikasi paparan. Dari sudut asas dan kejuruteraan, adalah wajar untuk menyiasat topik di atas. Dalam projek ini, filem nipis β-Ga_2O_3 yang disintesis oleh kaedah salutan putaran sol-gel dan fotoluminasinya telah disiasat. Untuk fabrikasi, keadaan pertumbuhan salutan putaran sol-gel, dan proses filem nipis β-Ga_2O_3 pada substrat Si dan Al_2O_3 telah disiasat. Rawatan khas pada substrat dan lapisan bersalut telah dijalankan untuk meningkatkan keseragaman dan kelicinan setiap lapisan bersalut dan filem termendap akhir. Kitaran salutan putaran dan suhu penyepuhlindapan yang berbeza juga disiasat dari aspek morfologi dan optik. Akhir sekali, satu set sampel dengan filem bersalut putaran 6 lapisan dan disepuhlindap di bawah suhu yang berbeza, iaitu dari 900 °C hingga 1100 °C telah disediakan. Sampel ini kemudiannya tertakluk kepada analisis pembelauan sinar-X secara mendalam. Keputusan menunjukkan bahawa mikro terikan bukanlah faktor utama untuk pelebaran puncak Bragg. Untuk menyiasat sifat luminasi, satu siri β-

Ga_2O_3 terdop Mo pada Al_2O_3 telah disintesis. Jalur luminasi hijau yang dikaitkan dengan peralihan jalur d_{xz}-d_{yz} ion Mo muncul perlahan-lahan dengan peningkatan kepekatan pengedopan Mo. Berbanding dengan β-Ga_2O_3 yang tidak didop, koordinat gambarajah kromatik CIE bagi Mo-doped β-Ga_2O_3 berubah daripada pancaran biru (0.222, 0.370) kepada pelepasan hijau (0.252, 0.507), dan kontras pancaran hijau adalah ketara. bertambah baik daripada 0.33 kepada 0.73.

SPIN COATED GALLIUM OXIDE THIN FILMS AND THE EFFECT OF Mo-DOPING CONCENTRATION ON LUMINESCENCE PROPERTIES

ABSTRACT

Beta-type gallium oxide (β-Ga_2O_3) with ultra-wide band gap energy and good emission property is suitable for optoelectronic applications such as luminescence devices. However, the growth of good quality β-Ga_2O_3 films using low cost and simple techniques, particularly the sol-gel spin coating technique, is still remains challenging. For luminescence features, undoped and doped β-Ga_2O_3 emit multicolour emissions due to the multi-energy level of intrinsic vacancies, which is unsuitable for the display application. From the fundamental and engineering point of view, it is worth investigating the above topics. In this project, the β-Ga_2O_3 thin films synthesized by the sol-gel spin coating method and their photoluminescence were investigated. For the fabrication, the sol-gel spin coating growth conditions, and processes of the β-Ga_2O_3 thin films on Si and Al_2O_3 substrates were investigated. Special treatments on the substrate and the coated layer were conducted to improve the uniformity and smoothness of each coated layer and the final deposited film. Different spin coating cycles, and annealing temperatures were also investigated from the morphologic and optical aspects. Finally, a set of samples with 6-layers spin-coated films and annealed under different temperatures, i.e., from 900 °C, to 1100 °C were prepared. These samples were then subjected to an in-depth X-ray diffraction analysis. The results show that the micro strain is not the key factor for the Bragg peaks broadening. To investigate luminescence properties, a series of Mo-doped β-Ga_2O_3 on Al_2O_3 were synthesized. A green luminescence band associated with the Mo ion d_{xz}-d_{yz} band transition appeared slowly with the increase of the Mo-doping concentration. As

compared with the undoped β-Ga_2O_3, the coordinate of the CIE chromaticity diagram of Mo-doped β-Ga_2O_3 changes from blue emission (0.222, 0.370) to green emission (0.252, 0.507), and the contrast of the green emission was significantly improved from 0.33 to 0.73.

CHAPTER 1

INTRODUCTION

1.1 Introduction

With the development of industry technology, semiconductor materials and devices have played an important role in our daily life, such as the computer, light emitting diode displays, and sensors (Nikolic et al., 2020; Todescato et al., 2016; Tricoli et al., 2010; Wang et al., 2018). Silicon (Si) is the first-generation semiconductor material, which is abundant on earth and easy to obtain. The thermal and mechanical properties of Si material are good for application as semiconductor materials (Diebold et al., 2001; Pavesi et al., 2010; Radziemska et al., 2003). All of these advantages make Si meet the needs of the electronics industry's development for the first several decades. However, with the development of the microelectronics industry, and according to Moore's Law (Mack et al., 2011; Theis et al., 2017; Thompson et al., 2006), Si material shows some limitations. For example, the low breakdown voltage and narrow band gap of Si make it difficult to be utilized in the device and applications with high frequency, high mobility, and high power (Ko et al., 2010; Meindl et al., 2001; Morton et al., 2011). Therefore, new generation semiconductor materials have been studied. As the second-generation semiconductor, indium phosphide, gallium arsenide, etc., with higher mobility and better optoelectrical properties (Jalali et al., 2022; Mushonga et al., 2012; Papež et al., 2021; Serpone et al., 2012), which suffice the requirement of high frequency, speed, and power device applications.

Over the past few decades, researchers are focused more on wide band gap semiconductors with an energy band gap (E_g) $\geqslant$ 2.0 eV (Takahashi et al., 2007;

Woods, 2020) because these semiconductors are the primary material for optoelectronic applications working from ultra-violet (UV) to visible spectral regions. For instance, wide band gap semiconductors have been widely utilized in light-emitting diode (LED), laser diodes, solar cells (Fujita, 2015; Fujita et al., 2016), visible and solar-blind sensors, transparent conducting electrodes, etc. (Dimopoulos et al., 2010; Kumar et al., 2019). Researchers have obtained the blue LED and laser diodes devices by gallium nitride (GaN, 3.4 eV) (Grodzicki et al., 2017; Pushpakaran et al., 2020) for several decades, which makes GaN become one of the representatives of the third-generation semiconductor material (Flack et al., 2016; Pane et al., 2019). Due to the wide band gap, good thermal stability, and high carrier saturation drift velocity, C is also used to manufacture various high-temperature, high-frequency, high-efficiency, and high-power devices (Hassan et al., 2018; Kim et al., 2012; Noh et al., 2016; Sun et al., 2020).

Compared to GaN, beta phase gallium oxide (β-Ga_2O_3) has a wider band gap (4.9 eV) (Mohamed et al., 2011; Rafique et al., 2017), which has more stable physical and thermal properties as well as better optoelectrical properties (Pearton et al., 2018; Zhang et al.,2020). The transmittance in the UV region reaches more than 80% (Qian et al., 2016), which makes up for the shortcomings of traditional transparent conductive films such as tin-doped indium oxide (ITO), tin oxide, and zinc oxide, which are opaque in the deep ultra-violet (DUV) region (Hrong et al., 2017), and thus has attracted widespread attention. Due to the oxygen vacancies, undoped β-Ga_2O_3 films usually exhibit n-type semiconductor behaviour (An et al., 2016; Dong et al., 2017). Hence, it is a very promising DUV transparent conductive thin film material.

For the synthesis of β-Ga_2O_3, metalorganic chemical vapor deposition (MOCVD) and molecular beam epitaxy (MBE) are commonly used (Du et al., 2015; Sasaki et al., 2013). Apart from these advanced synthesis techniques, sol-gel method is also used for synthesizing metal oxides thin film (Thiagarajan et al., 2017). Generally, the sol-gel method involves the formation of a sol through hydrolysis and polymerization, followed by the formation of a rigid porous gel. The final product (metal oxide thin film) is often obtained by removing the solvent from the gel by aging, drying, and annealing (Ugemuge et al., 2021). Spin coating is the most used sol-gel method for preparing the thin film from the sol-gel (Al-Agel et al., 2012; Kamaruddin et al., 2011; Nistico et al., 2017). Compared to the MOCVD and MBE methods, sol-gel spin coating has many advantages, i.e., low processing temperature, no vacuum condition required, easy composition control, large coating area, good reproducibility, low equipment cost, and environment friendly (Sahu et al., 2009; Tyona, 2013). Hence, it is worth exploring and studying the sol-gel spin-coating growth of undoped and doped β-Ga_2O_3 thin films on various substrates.

Since, for the spin coating process, the composition is easy to control, the doped β-Ga_2O_3 is possible to be obtained by spin coating. One application of the doped semiconductor material is as the luminescence device. Furthermore, as a wide band gap material, β-Ga_2O_3 is a good host material for improving the efficiency of the emission obtained from the doped ions (Shinde et al., 2014; Wu et al., 2015; Zavada et al., 1995). For the undoped β-Ga_2O_3, generally, a multiband emission can be obtained, i.e., UV emission, blue emission, and green emission (Mi et al., 2013; Nie et al., 2022). With the different dopants, the doped β-Ga_2O_3 will generate more color emission bands, such as yellow, orange, and red emissions (Deng et al., 2021; Gonzalo et al., 2014; Naresh et al., 2021; Wellenius et al., 2008). However, as mentioned above,

the wide band gap β-Ga_2O_3 always emits multicolor emissions (Tadjer et al., 2019; Zhang et al., 2005). But individual color emission is also necessary. Therefore, finding a way to obtain an individual color emission from β-Ga_2O_3 is also crucial for optoelectronic applications.

1.2 Motivation and problem statements

Compared to MOCVD and MBE, the sol-gel spin coating growth of undoped and doped β-Ga_2O_3 thin films are relatively cheap, simple, and environment friendly (Lee et al., 2017). However, the sol-gel spin coating growth of undoped and doped β-Ga_2O_3 thin films have not yet been fully investigated. For example, the effects of substrate's pre-treatment (i.e., substrate cleaning with piranha solution and heat treatment of the coated layer) on the sample's morphology, thickness, and structure quality remain unclear. Therefore, for future application, such as the photodetector and luminescence device (Chen et al., 2018; Oh et al., 2017), the surface morphology and crystalline quality of the spin-coated β-Ga_2O_3 thin films need to be improved.

For the sol-gel spin coating process, the type and amount of the precursors (source material and dopant) can be easily controlled in the preparation process. However, it is hard to control the incorporation of the dopant into the β-Ga_2O_3 crystal matrix. In other words, it is quite challenging to dope the β-Ga_2O_3 using the sol-gel spin coating method, and many fundamental issues remain unclear.

As mentioned previously, under the premise of good crystalline quality and smooth surface morphology, wide band gap materials are also good host materials for luminescence applications (Wu et al., 2015; Zavada et al., 1995). Nevertheless, the effect of doped ions on the luminescence mechanism is also unclear. For β-Ga_2O_3, it generally emits multicolor emissions. Hence, this behavior makes it not suitable for

some optoelectronic applications, such as the red, green, and blue (RGB) display system. From the engineering point of view and the RGB display applications, obtaining single color emission from β-Ga_2O_3 is important. Amongst these three colors of the RGB system, the green color emission is difficult to obtain due to the lack of direct band gap materials with a band gap energy of around 2.6 eV (Assali et al., 2013). In order to obtain a narrow green color emission from β-Ga_2O_3, a better understanding of its mechanism is also crucial.

In summary:

1. The substrate and coated layer hydrophilia need to be enhanced to improve surface morphology and crystalline quality.

2. It is needed to obtain the doped β-Ga_2O_3 via the sol-gel spin coating method with a smooth surface for the photoluminescence application.

3. No research relates to the individual green color photoluminescence obtained from doped β-Ga_2O_3.

1.3 Scope of work and research objectives

This project mainly focuses on the sol-gel spin coating growth and characterization of undoped and doped β-Ga_2O_3 thin films. For the doping studies, the β-Ga_2O_3 was doped with different Mo-doping concentrations. For the synthesized undoped and doped β-Ga_2O_3 thin films, their structural, surface morphological, optical properties were investigated. For doped β-Ga_2O_3 thin films, special attention was paid to the investigation of its photoluminescence property and the luminescence mechanism.

Typically, for sol-gel spin coating growth, the surface morphology and crystalline quality can be improved by enhancing the hydrophilicity of the substrate and the coated layer. The hydrophilicity of the substrate can be improved through the pre-treatment of the substrate, while that of the coated layer can be enhanced through the heat treatment process. Hence, the first objective was to investigate the effects of pre-treatment of the substrate using piranha solution and heat treatment of the coated layer on the spin coated β-Ga_2O_3 thin films on p-Si substrate. Subsequently, a series of spin coated β-Ga_2O_3 thin films on p-Si substrate were prepared, and optimization works on the annealing temperature and spin coating cycles were carried out. Then the fundamental properties of the spin-coated β-Ga_2O_3 on the p-Si substrate were characterized to check the quality of the synthesized β-Ga_2O_3 thin film from both surface smoothness and crystal quality, which include the X-ray Diffraction (XRD), Fourier-transform infrared spectroscopy (FTIR), UV-Visible Spectroscopy (UV-Vis), field emission scanning electron microscopy (FESEM), and atomic force microscopy (AFM). The XRD results were further deeply analysed by Williamson-Hall and size-strain plots methods for the β-Ga_2O_3 with various annealing temperature to characterize the difference of the crystal features with different annealing temperature.

For the doped β-Ga_2O_3 sample, the molybdenum (Mo) was used as the dopant. A series of sol-gel spin coated Mo-doped β-Ga_2O_3 samples with different doping concentrations were grown on sapphire substrate. Then, the effects Mo-doping concentration on the properties of the doped β-Ga_2O_3 thin films were analysed by XRD technique and UV-Vis spectroscopy. Since the effect of doped ions on the green color luminescence mechanism of the doped β-Ga_2O_3 remains unclear, the last objective was paid to the investigation on the effects of Mo-doping concentration on the

luminescence property and the mechanism behind of the Mo-doped β-Ga_2O_3 thin films.

In summary, the main objectives of this project are listed as follows:

1. To investigate the effects of pre-treatment of the substrate using piranha solution and heat treatment of the coated layer on the crystalline quality of the spin coated β-Ga_2O_3 thin films on p-Si substrate.

2. To investigate the sol-gel spin coating growth of Mo-doped β-Ga_2O_3 thin films on sapphire substrate with different Mo-doping concentrations.

3. To investigate the effects of Mo-doping concentration on the narrow green color photoluminescence properties of the Mo-doped β-Ga_2O_3 thin films and the mechanism behind.

1.4 Originality

For the sol-gel spin coating growth of β-Ga_2O_3 thin films on p-Si substrate, a series of experiments for the pre-treatment of the uncoated p-Si substrate and the heat treatment of coated layer were conducted to improve both the crystal structure and surface smoothness. A patent based on the pre-treatment experiment was successfully filed. For the first time, the β-Ga_2O_3 thin films on p-Si substrate with different annealing temperatures were deeply analysed by the Williamson-Hall and size-strain plots to verify the crystalline quality of the coated films.

For the sol-gel spin coating growth of doped β-Ga_2O_3, Mo element was used as the dopant for the first time. The XRD patterns, UV-Vis transmissivity, band gap energy, and surface morphology of the coated films were investigated thoroughly.

Through this work, Mo-doped β-Ga_2O_3 thin films with high contrast narrow green color emission was obtained for the first time, and its luminescence mechanism was proposed.

1.5 Dissertation organization

The content of this thesis was organized into several chapters, which begin with a brief introduction and research objectives.

Chapter 2 introduces the fundamental properties of the β-Ga_2O_3, which include the structural, optical, and electrical properties. The luminescence properties of the doped β-Ga_2O_3 with different dopant were reviewed in detail. Besides the properties of β-Ga_2O_3, the commonly used synthesis techniques were introduced briefly. However, the sol-gel spin coating method was reviewed thoroughly. This includes the mechanism of the spin coating method and the literature review of the relative works of the synthesis of undoped and doped β-Ga_2O_3 by sol-gel spin coating method. Furthermore, the effect of different treatments on the substrate for the spin coating process was reviewed.

Chapter 3 describes the research methodologies used in this project. For the experiment works, the specific steps and operations were presented. This includes the preparation of the precursor and substrate, substrate pretreatment, and the details of the spin coating process. A series of characterization methods were also introduced.

Chapter 4 presents the optimization results of the sol-gel spin-coated β-Ga_2O_3 thin films on p-Si substrate prepared under different synthesis parameters. Williamson-Hall and size-strain plots methods that used to assess the structural quality of β-Ga_2O_3 thin films were also discussed.

Chapter 5 is the results and discussion of the sol-gel spin coating growth and characterization of Mo-doped β-Ga_2O_3 thin films. The XRD patterns of the undoped and Mo-doped β-Ga_2O_3 were analysed and discussed. The effects of Mo concentration on the energy bandgap and luminescence properties were also investigated. For the photoluminescence, a green color emission was obtained, and the mechanism behind was discussed.

Chapter 6 is the summarised conclusions of the whole object and the recommendations for the future study.

CHAPTER 2

LITERATURE REVIEW

2.1 Introduction

Wide band gap semiconductor materials have attracted much attention for their applications in optoelectronic devices, such as UV photodetectors (Jokinen et al. 2012; Rai et al., 2015; Zhang et al., 2018), light-emitting diodes (Kim et al., 2017; Shur, 2019), and lasers (Chowdhury et al., 2005). Gallium oxide (Ga_2O_3), especially for the beta phase (β-), is a semiconductor with a wide band gap around 4.9 eV (Matsuzaki et al., 2006; Rafique et al., 2017). It has high mechanical strength, UV transparency, and high chemical stability (Kumar et al., 2019; Oh et al., 2017), which also attracted many interests. This chapter presents the fundamental properties of the Ga_2O_3, especially for the β-Ga_2O_3 thin film. Special attention was paid to the luminescence of doped β-Ga_2O_3. For the fabrication process, in addition to the sol-gel spin coating method, other common synthesis methods for β-Ga_2O_3 are briefly reviewed. For the spin coating process, the treatment of the substrate is reviewed thoroughly.

2.2 Fundamental properties of undoped/doped β-Ga_2O_3 thin films

2.2.1 Structure properties

There are numerous polymorphs of Ga_2O_3, which are labelled as α-, β-, γ-. δ-, ε-, and κ (Pearton et al., 2018; Swallow et al., 2020). All these different Ga_2O_3 polymorphs can be synthesized under particular conductions and transferred to the most thermodynamically stable β-Ga_2O_3 phase with varying treatment conditions (Pearton et al., 2018; Swallow et al., 2020), as shown in Figure 2.1.

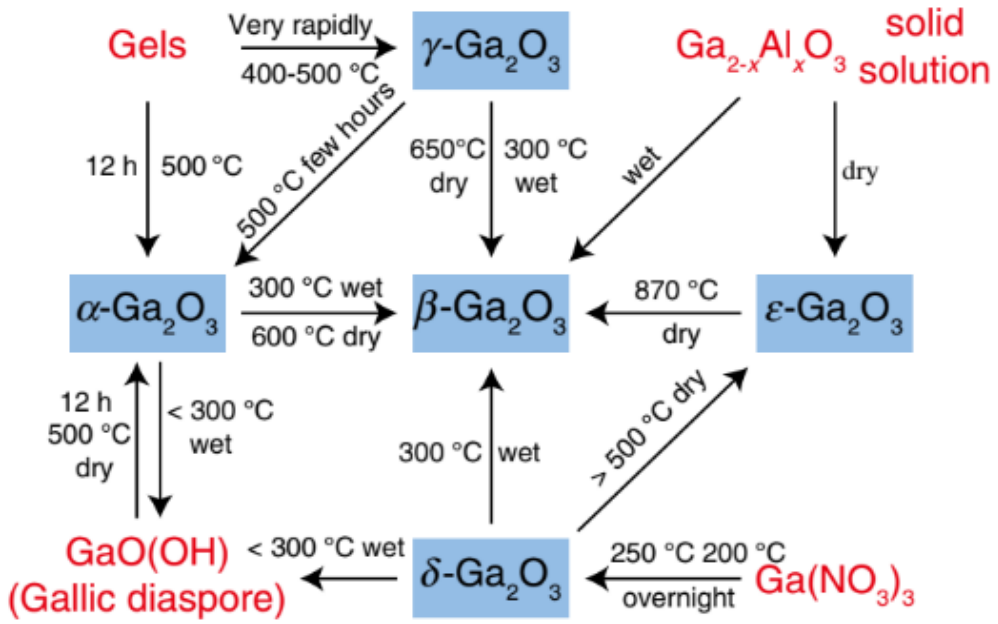

Figure 2.1 Transformation relationships among the different polymorphs of Ga_2O_3 (Roy et al., 1952).

The α-Ga_2O_3 is a metastable polymorph, which has a rhombohedral structure and belongs to space group $R\bar{3}c$ (Guo et al., 2016) and analogous to corundum (sapphire, α-Al_2O_3). The band gap of α-Ga_2O_3 is around 5.3 eV (Akaiwa et al., 2012; Fujita et al., 2016). It can be synthesized by heating GaO (OH) at about 500 ℃ in air ambient. The second phase, namely, the most stable β-Ga_2O_3, has a monoclinic structure, which belongs to the space group $C2/m(C_{2h}^3)$ (Mohamed et al., 2019; Peelaers et al., 2015), the reported band gap of β-Ga_2O_3 is around 4.9 eV (Matsuzaki et al., 2006; Rafique et al., 2017). The β-Ga_2O_3 can be transformed by any other polymorphs of Ga_2O_3 at sufficiently high temperatures in the air atmosphere (Pearton et al., 2018; Playford et al., 2013). The third phase, γ-Ga_2O_3 has a defective cubic spinel-type structure ($MgAl_2O_4$-type) with the space group $Fd\bar{3}$. Its band gap is about 5.0 eV and 4.4 eV for direct and indirect band gap, respectively (Oshima et al., 2012). The ε-Ga_2O_3 was first synthesized in 1952 (Roy et al., 1952), which has a cubic defect spinel structure, such as γ-Al_2O_3. The space group of ε-Ga_2O_3 is $P6_3mc$ (Playford et

al., 2013) and its band gap is around 5.0 eV and 4.5 eV for direct and indirect band gap, respectively (Nishinaka et al., 2016). Table 2.1 summarizes the structural properties of the Ga_2O_3 polymorphs.

Table 2.1 The basic parameters of Ga_2O_3 polymorphs

Polymorph	Structure & space group	Lattice parameters (Å)	Band gap (eV)	Reference
α	rhombohedral $R\bar{3}c$	a =4.9825± 0.0005 c=13.433 ±0.001	5.3	(Guo et al., 2016; Shinohara et al., 2008)
β	monoclinic $C2/m$	a=12.23 ± 0.02 b = 3.04 ± 0.01 c=5.80 ± 0.01 β = 103.7 ± 0.3	4.4–5.0	(Geller, 1960; Onuma et al., 2015)
γ	cubic $Fd\bar{3}m$	a=8.30 ± 0.05	4.4 (indirect) 5.0 (direct)	(Areán et al., 2000; Oshima et al., 2012)
δ	cubic $Ia\bar{3}$	a=10.00	-	(Roy et al., 1952)
ε	hexagonal $P6_3mc$	a=2.9036 c=9.2554	4.9 (direct) 4.5 (indirect)	(Oshima et al., 2015a, 2015b) (Nishinaka et al., 2016)

As mentioned above, the most stable polymorph of Ga_2O_3 is the β-phase, making it the most common and well-studied one. The lattice of β-Ga_2O_3 was first reported by Kohn et al. (Kohn et al., 1957), and the structure was determined by Geller (Onuma et al., 2015), which classified the β-Ga_2O_3 into space group C2/m. The most recent and accurate study of the crystal structure of β-Ga_2O_3 was reported by Ahman et al. (Åhman et al., 1996), which shows the same space group but about 10 times better than the previous works. Figure 2.2 shows the unit cell of β-Ga_2O_3. There are two crystallographically inequivalent Ga positions, which are labeled as Ga (I), the tetrahedral geometry, and Ga (II) the octahedral geometry. Three different oxygen O (I), O (II), and O (III) are arranged in a “distorted cubic” close-packed array, in which two atoms are coordinated trigonally, and one is coordinated tetrahedrally.

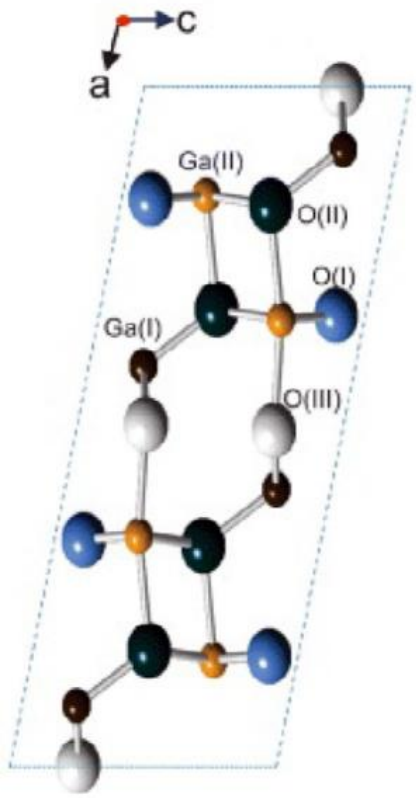

Figure 2.2 Unit cell of β-Ga_2O_3 and the two inequivalent Ga (I) and Ga (II), three inequivalent O (I), O (II) and O (III) (Stepanoc et al., 2016).

Due to the anisotropy of the crystalline, the thermal conductivity of β-Ga_2O_3, changes a lot along different crystal direction. The largest thermal conductivity occurs along the [110] direction, while the lowest is along the [100] direction, which is 27 W/mK (Guo et al., 2015), and 10.9W/mK (Guo et al., 2015), respectively, as shown in Table 2.2. Some other physical properties of β-Ga_2O_3 are shown in Table 2.3.

Table 2.2 Thermal conductivity of β-Ga_2O_3 with different crystal orientation.

	Thermal conductivity	Reference
[100]	10.9 ± 1.0 W/mK	(Guo et al., 2015)
	13 W/mK	(Víllora et al., 2008)
[-201]	13.3 ± 1.0 W/mK	(Guo et al., 2015)
[001]	14.7 ± 1.5 W/mK	(Guo et al., 2015)
[110]	27.0 ± 2.0 W/mK	(Guo et al., 2015)
[010]	21.0 W/mK	(Galazka et al., 2014)

Table 2.3 Other physical properties of β-Ga_2O_3.

Property	Value	Reference
Density	5.59 g/cm3	(Víllora et al., 2016)
Melting point	1795 ℃	(Víllora et al., 2008)
	1795 ±15℃	(Schneider et al., 1963)
	1740 ℃	(Rai et al., 2015)
Specific heat	0.56 $Jg^{-1}K^{-1}$	(Galazka et al., 2014)
	0.49 $Jg^{-1}K^{-1}$	(Víllora et al., 2016)

2.2.2 Optical properties

Pure β-Ga_2O_3 is colorless and highly transparent in the ultraviolet range since its wide band gap energy (Okada et al., 2022; Zhang et al., 2006). However, impure or doped β-Ga_2O_3 as well as undoped β-Ga_2O_3 synthesized under some specific conditions, such as annealed in reducing or no-reducing conditions, will show some colors (Galazka et al., 2014, 2010). The light-yellow color of β-Ga_2O_3 is attributed to some weak absorption in the blue range of the visible spectrum. For n-type β-Ga_2O_3, it shows bluish color due to the increased free carrier absorption in the red and near-infrared (NIR) regions of the spectrum. Grey color is original from the impurities, such as carbon. The free electron concentration is also a key factor that affects the color and transmittance spectra of β-Ga_2O_3 (Galazka et al., 2014), as shown in Figure 2.3. However, there is an absorption edge at around 255-260 nm of all these different samples shown in Figure2.3, which is attributed to the transition from the valence band to the conduction band of the β-Ga_2O_3 (Zhang et al., 2006). For samples with low electron concentration, they exhibit good transparency in the visible and NIR region (Matsuzaki et al., 2006). As the electron's concentration increases gradually, the transmittance first decreases in the NIR region and then in both NIR and visible range with a very high free electron concentration. The absorption edge also depends on the polarization of incident light (Sun et al., 2020; Ueda et al., 1997; Ricci et al., 2016).

The absorption edges for $E||a$, $E||b$, and $E||c$ are 4.34 eV, 4.81 eV, and 4.54 eV, respectively (Sun et al., 2020; Ueda et al., 1997). These different polarization-sensitive absorption edges contribute to the direct optical transitions between different valence band levels and conduction band levels that are dipole allowed for $E||a$, $E||b$, and $E||c$ (Galazka, 2018).

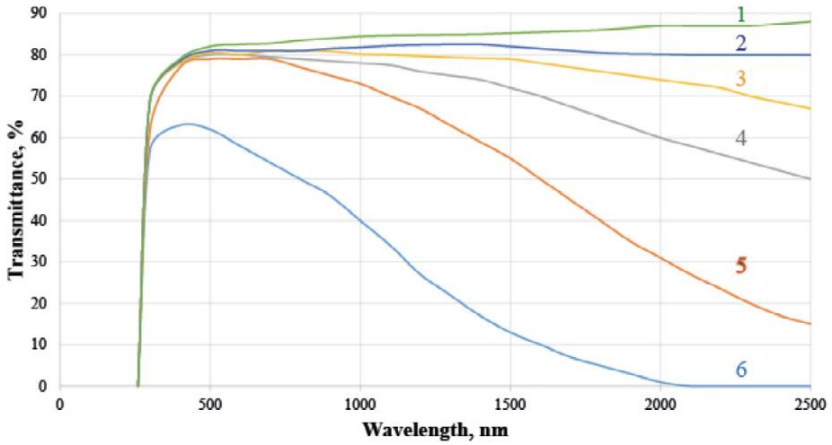

Figure 2.3 Transmittance spectra of as-grown β-Ga_2O_3 with various free electron concentrations: 1- insulating (doped with Mg); 2: 4×10^{16} cm^{-3}; 3: 3.5×10^{17} cm^{-3}, 4: 5.2×10^{17} cm^{-3}, 5: 2.2×10^{18} cm^{-3}; 6: 1×10^{19} cm^{-3} (doped with Sn) (Galazka et al., 2014).

For the luminescence properties, there is no near band edge emission shown in the photoluminescence (PL) spectra of pure β-Ga_2O_3 (Ohira et al., 2008). But pure β-Ga_2O_3 exhibits multiband emissions, for example, UV (3.2-3.6 eV), blue (2.8-3.0 eV), and green (2.4 eV) emission bands (Wang et al., 2018; Guzman et al., 2011; Chen et al., 2016). The UV emission band was originated from the recombination between free electrons and the self-trapped holes (Varley et al., 2012). The blue emission band was related to the oxygen vacancies, which were also responsible for the n-type conductivity of Ga_2O_3 (Onuma et al., 2013). The blue emission could also be originated from the recombination of the self-trapped hole and the electron trapped at a single oxygen vacancy (Dong et al., 2017; Harwig et al., 1978; Yamaga et al., 2011).

Harwig et al. (1978) pointed out that the possible donors are V_O and Ga^{3+}, and possible acceptors are V_{Ga} and/or V_O-V_{Ga} pairs. The green emission occurs via the recombination of a self-trapped hole and an electron trapped at a cluster of oxygen vacancies (Yamaga et al., 2011). Some researchers also found that the intensity of blue emission decreases when doped with transition metals (Nakazawa et al., 2013).

In addition to these original emission bands, there are some other emission bands. Table 2.3 summarizes the luminescence properties of β-Ga_2O_3 with different parameters, such as the type of substrates, synthesis methods, dopants, and the type of nanostructures. For undoped β-Ga_2O_3, both the substrate and synthesize method will affect the emissions. For the same synthesis method and substrate, the dopant will influence the emission directly, as the items of (Su et al., 2019) and (Wu et al., 2015) shown in Table 2.3. Deng et al. (2021), Chen et al. (2016), and Wellenius et al. (2008) found that with the same synthesis method, and dopant element, different substrates will also affect the emission. It was also reported that β-Ga_2O_3 doped with different dopants would emit colors such as yellow, orange, red, and longer wavelength emission bands (Deng et al., 2021; Makeswaran et al., 2021; Shi et al., 2010; Wellenius et al., 2008; Wu et al., 2015; Zhao et al., 2011), as shown in Table 2.3. Furthermore, with the new color emissions appearance, some of the original color emissions disappeared. However, no matter the synthesis method, substrate, and dopant type, most of the emissions are multicolor.

Table 2.4 Luminescence properties of β-Ga_2O_3 with different conditions.

No.	substrate	method	dopant	Band gap (eV)	Emission position (wavelength/nm)				Structure	Reference
					UV	Blue	Green	Others		
1	Si	PLD[##]	amorphous	4.3	-	-	506	Orange:622	film	(Makeswaran et al., 2021)
			crystalline	4.7			502	Orange:597		
2	quartz	Thermal evaporation	-	4.7.-5.13	300	400 438	-	-	film	(Shi et al., 2019)
3	Al_2O_3, Au	-	-	-	316, 370	419,452,480	510	-	wire	(Chang et al., 2004)
4	MgAl6O10	MOCVD[*]	-	-	369	412, 464	534	-	film	(Mi et al., 2013)
5	$NiCl_2$-coated Si	CVD[**]	Sn	-	354	416 471	518	-	film	(Wei et al., 2016)
			Eu/Er×150[+]	-	-	-	505, 524	Red:611, 665	film	
6	Al_2O_3	PLD	Eu	-	-	-	-	Red:611	film	(Deng et al., 2021)
			Er	-	-	-	505, 524	Red: 665	film	
7	Si	PLD	Er	4.9	-	-	524,533,548,559	-	film	(Chen et al., 2016)
8	Al_2O_3	RF sputtering	-	4.96	258, 290, 346, 378				film	(Su et al., 2019)
			Zn	4.88	399	421, 445	-	-	film	
			Zn/Mg	5.08	307,399				film	
9	Al_2O_3	RF sputtering	Nd	4.61-4.93	-	-	-	905,1067,1339	film	(Wu et al., 2015)
10	ATO+ITO	PLD	Eu	-	-	-	-	Oramge:589 Red:611, IR: 778	film	(Wellenius et al., 2008)
11	BPGG[#]	-	Tm	-	-	-	-	1465, 1800	film	(Shi et al., 2010)
12	Al plate/Si	Electrospinning	Tb	-	-	491	550	Orange:591, Red: 625	fibre	(Zhao et al., 2011)

[##]BPGG: Bi_2O_3(PbO)–GeO_2–Ga_2O_3 glass; [##]PLD: pulsed laser deposition: [*]MOCVD: metal organic chemical vapor deposition; [**]CVD: chemical vapor deposition; [+]Eu/Er × 150: the double layer structure repeated 150 times.

Generally, the red, green, and blue (RGB) emissions are much more important than other emission colors since the RGB color model is the primary color for the display applications (Fröbel et al., 2018). Both the red and blue colors can be obtained from the direct emission band (Yang et al., 2004; Yang et al., 2011; Zhong et al., 2012). Due to the lacking of the material with a direct band gap around 2.2-2.4 eV, there are a few semiconductors that have a band gap energy corresponding to green light (Assali et al., 2013), and presents a specific fundamental problem (Desnica, 1998; Li et al., 2011; Nakamura, 2009; Oh et al., 2012). From Table 2.3, it can be seen that green emission can be obtained from the doped β-Ga_2O_3. However, the green color emission consisted of multi-emission bands. For instance, the green color emission from the Er-doped β-Ga_2O_3 composed of four emission bands, i.e., 524 nm, 533 nm, 548 nm, and 559 nm (Chen et al., 2016). Clearly, narrow green emission band from doped β-Ga_2O_3 is still challenging.

2.2.3 Electrical properties

The electronic structure of β-Ga_2O_3 was investigated theoretically and experimentally. For theoretical methods, the density functional theory (DFT) and hybrid functional (HDF) were used (Pourshahrestani et al., 2016; Zhou et al., 2014). Since the DFT is based on the ground state theory, which underestimates the exchange-correlation potential among the excited electrons, it tends to underestimate the band gap values (Mock et al., 2017). HDF is a more accurate method, and the obtained results are much better in agreement with the experiment results (Peelaers et al., 2015; Playford et al., 2013). Most of the results concluded that the Γ point (the Brillouin zone center) is the conduction-band minimum of β-Ga_2O_3, and the balance band is flat. However, for the position of the valence band maximum, researchers give different opinions. He et al. (He et al., 2006) pointed out that the balance band maxima occurs

almost degenerated at the Γ and M k-points, at which there is a direct gap of 4.69 eV at Γ and an indirect M-Γ gap of 4.66 eV. Varley et al. (2010) found that the valence band maximum is near the M point. This resulted in an indirect band gap of 4.83 eV, slightly smaller than the direct band gap of 4.87 eV at Γ point. Peelaers et al. (2015) pointed out that the fundamental indirect band gap of β-Ga_2O_3 is 4.84 eV. The valance band maximum is located at I-L line, which makes the direct band gap at Γ is 4.88 eV. From all these results, the small difference between the indirect and direct band gaps makes β-Ga_2O_3 a direct band gap material, which was experimentally measured at ~ 4.9 eV (Varley et al., 2010). However, the band gap is not fixed, especially with doping. The band gap can decrease due to the narrow effect (Luo et al., 2002; Zheng et al., 2000), in which the band tail and impurity band extended as the doping concentration increased. Subsequently, this makes the band tail and impurity band overlap. With heavy doping concentration, the band gap can also arise caused by Moss-Burstein (Manjunatha et al., 2018; Saw et al., 2015). As the states adjacent to the conduction band become occupied, the absorption edge is pushed towards higher energies, increasing in the apparent band gap of a semiconductor.

For calculation with different conditions, for example, at or in the vicinity of the Γ point of the Brillouin zone, the calculated m_e^*/m_0, where m_e^* and m_0 is the effective electron mass and the electron mass of the β-Ga_2O_3, which are 0.220-0.300 (Mock et al., 2017), 0.227-0.242 (Yamaguchi, 2004), 0.260-0.270 (Furthmüller et al., 2016), 0.280 (Varley et al., 2010), 0.342 (Dong et al., 2017), respectively. Compared to the calculated results, the experimental results of the effective electron mass show an anisotropy feature. For instance, for (010) plane, the value of m_e^*/m_0 are 0.283-0.288 (Janowitz et al., 2011; Mohamed et al., 2010); for the $(\bar{2}01)$ plane, the value of m_e^*/m_0 are 0.276-0.311 (Knight et al., 2018). The maximum electron mobility of bulk

β-Ga_2O_3 measured at room temperature is 152 cm^2/Vs (Galazka et al., 2014) and 172 cm^2/Vs (Onuma et al., 2015). However, since electron mobility is a function of the free electron concentration, for good quality crystals, the electron mobility changed a lot when the concentration changed from 2×10^{16} to 5×10^{20} cm^{-3} (Baldini et al., 2016; Lee et al., 2016; Sasaki et al., 2012) as shown in Figure 2.4. Thereby, it can be concluded that the electron mobility decreases as the concentration increases. However, the electron mobility is much lower for the crystals with poor quality or layer structure. The low electron mobility of the layer structure can only be measured at very high dopant concentrations (generally above 10^{18} cm^{-3}), and the mobility drops rapidly below this doping level, as Figure 2.4c shown (Baldini et al., 2016; Lee et al., 2016; Sasaki et al., 2012). This behavior is explained by the lateral incoherent twin boundaries (ITB) mode (Fiedler et al., 2017; Schewski et al., 2016), in which there is a dangling bond in each unit cell that acts as an acceptor-like electron trap. After electrons are trapped by dangling bonds, negatively charged regions are formed, which causes the valence and conduction band edges to bend and act as charge barriers. (Yamaguchi, 2004). Table 2.4 summarizes the basic electric properties of β-Ga_2O_3.

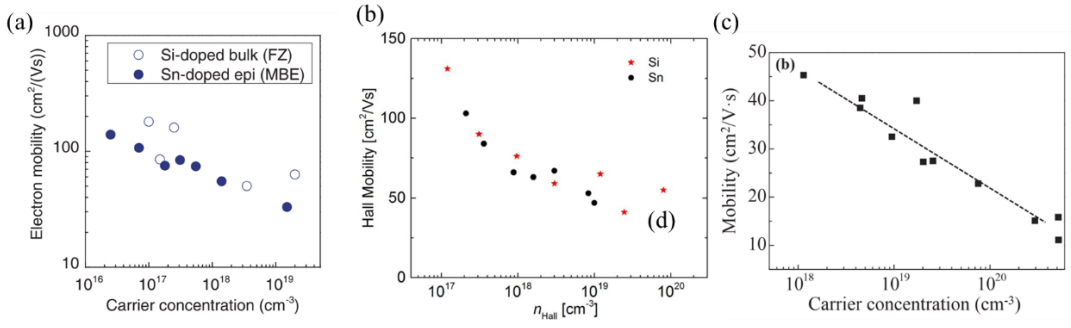

Figure 2.4 (a) Electron mobility as a function of a carrier concentration of optical floating zone (OFZ) and MBE formed Si-and Sn-doped layers (Sasaki et al., 2012). (b) Hall mobility values function as carrier density for Si- and Sn-doped layers (Baldini et al., 2016). (c) relationship between mobility and carrier concentration for Sn-doped films (Lee et al., 2016).

Table 2.5 Basic electric properties of hetero- and homo-epitaxially grown β-Ga_2O_3 by different epitaxial techniques.

Epitaxial technique	Dopant	Electron concentration [cm^{-3}]	Electron mobility [$cm^2V^{-1}s^{-1}$]	Substrate	Reference
MOVPE*	Si Sn	$1\times10^{17} – 8\times10^{19}$ $4\times10^{17} – 1\times10^{19}$	50-130	β-Ga_2O_3 (100)	(Baldini et al., 2016)
MBE**	Sn	$2\times10^{16} – 1\times10^{19}$	120	β-Ga_2O_3 (100)	(Sasaki et al., 2012)
MBE	Sn	$1\times10^{17} – 1\times10^{18}$	10-80	β-Ga_2O_3 (100)	(Okumura et al., 2014)
MOCVD	Sn	1×10^{18}	12	β-Ga_2O_3 (100)	(Du et al., 2015)
MOCVD	Sn	$5\times10^{17} – 2\times10^{18}$	10-41	β-Ga_2O_3 (100)	(Baldini et al., 2016)
MOCVD	Sn	$3.7\times10^{19} – 2.4\times10^{20}$	0.74-3.4	MgO	(Mi et al., 2015)
PLD#	Si	$2.6\times10^{19} – 1.7\times10^{20}$	19-27	β-Ga_2O_3 (100)	(Leedy et al., 2017)
PLD	Si	9.1×10^{19}	0.1-5.5	Al_2O_3 (0001)	(Zhang et al., 2015)

*MOCVD: metal organic chemical vapor deposition; **MBE: molecular beam epitaxy; #PLD: means pulsed laser deposition.

β-Ga_2O_3 is also a promising material for power device due to its wide band gap (Higashiwaki, 2021; Tadjer, 2018). However, to realize this application, it is necessary to form the effective n- and p-type doping. The undoped β-Ga_2O_3 is usually the n-type since the unavailable oxygen (O) vacancies in the material during fabrication (Dong et al., 2017). However, Varley (Varley et al., 2010) found that the O vacancies are deep donors, which cannot be a source of the conductivity but can be the source of luminescence. Therefore, the new impurities need to be induced to change the conductivity. Hydrogen (H) is the commonly used impurity to form the n-type β-Ga_2O_3 (Ritter et al., 2018; Varley et al., 2011; Venzie et al., 2022). The impurity of H can act as the donor by the interstitial species and substitutional donor on the oxygen site

(Varley et al., 2010). Some other comments can also be used as shallow donors, such as silicon (Si), tin (Sn), germanium (Ge), and fluorine (F) (Polyakov et al., 2018; Rafique et al, 2018; Ranga et al., 2021; Yan et al., 2016). The Si, Sn, and Ge impurities can be incorporated on the gallium site to form shallow donors (Zhang et al., 2010). For F, it can be from the shallow donor with an O site (Varley et al., 2010). For the hole in β-Ga_2O_3, since the self-trap in β-Ga_2O_3, there is no free hole, which the holes are more stable localized. From the theoretical studies, there is no p-type conductivity by the conventional doping methods (Ingebrigtsen et al., 2018; Kyrtsos et al., 2018; Li et al., 2012; Lyons, 2018; Varley et al., 2012) since all acceptor are too deep to form the free holes. Therefore, the incorporating acceptor impurities are possible to form the p-type β-Ga_2O_3. Peelaers (Peelaers et al., 2019) considered the N impurity incorporated on the O site, and Mg incorporated on the Ga site. Ritter (Ritter et al., 2018) considered the Mg-H complexes to form the p-type β-Ga_2O_3.

2.2.4 Remarks

Among the various phases, the β-Ga_2O_3 is the most stable phase. β-Ga_2O_3 is a monoclinic crystal structure that has a direct wide band gap energy of around 4.9 eV. The color of undoped pure β-Ga_2O_3 is almost transparent. With different impurities and dopants, the β-Ga_2O_3 exhibits some light yellow or grey color. As the concentration of electrons increases, the transmission of β-Ga_2O_3 decreases gradually. For luminescence properties, undoped and doped β-Ga_2O_3 emit multicolor emissions from UV to green. With some dopants and synthesis conditions, other color can also be emitted. Both the thermal conductivity and effective electron mass of β-Ga_2O_3 show anisotropy in different directions. The electron mobility also reduced with the concentration increased. But the electron mobility of layer structure is difficult to be measured unless the electron concentration is higher than 10^{18} cm^{-3}.

2.3 Growth of β-Ga_2O_3 thin film

From the literature review in the earlier section, different synthesis methods and processes will influence the quality and properties of the synthesized β-Ga_2O_3 thin film. In the next section, different synthesis techniques for Ga_2O_3 thin film will be briefly reviewed. But special attention will be paid to the sol-gel spin coating technique as this method was applied in this research work.

2.3.1 Chemical vapor method

Metal organic chemical vapor deposition (MOCVD) is the most used technique for the growth of Ga_2O_3 thin film. It is a kind of chemical vapor deposition (CVD) method, which uses the chemical reaction (in the gas phase) of the metal organic precursors with the aim element to form the targeted thin film on the substrate. For the Ga_2O_3 thin film, trimethylgallium (TMGa, $Ga(CH_3)_3$) or triethylgallium (TEGa, $Ga(C_2H_5)_3$) are commonly used with a carrier gas of Ar or N_2. For the O source, O_2, O_3, and O are typically used. According to (Baldini et al., 2014), H_2O is also used as the O source and produces good results. Wagner et al. (2014) and Gogova et al. (2014) found that when the TMGa was used, it was much better to use O_2 and H_2O as the O source than use H_2O only. Because the mixed O precursors can promote a smooth layer as compared to using a single O source where a rough layer with nanowires or agglomerates tends to produce. If only O_2 was used, there would create a $Ga_2(CO_3)_3$, which acts as a mask on the substrate, since the concentration H_2O are comparable with the concentration of CO_2 from TMGa, which will form the $Ga_2(CO_3)_3$. When the H_2O is used as the O source at the same time, the concentration of H_2O will be much higher than the CO_2 and absorb the CO_2, while H_2O will promote the growth of monocrystalline layers since it will dissociate at oxygen vacancy sites. MOCVD method is applied to grow β-Ga_2O_3 both heteroepitaxially and homoepitaxially. The

β-Ga_2O_3 substrate with (100), (010), and (001) orientations were produced through the homoepitaxial growth. But for the heteroepitaxial grown β-Ga_2O_3 layer, the structure quality is relatively poor as they are generally amorphous or polycrystalline. Al_2O_3 (0001) are always used as the heteroepitaxial substrate (Schewski et al., 2014). For this substrate, during the deposition process, a layer of α-Ga_2O_3 is first grown and then converted into relaxed β-Ga_2O_3 with ($\bar{2}$01). For the doped β-Ga_2O_3 film, Si and Sn are typically used via the metal organic precursors of tetraethyl orthosilicate (TEOS, Si($OC_2H_5)_4$)), and tetraethyltin (TESn, $Sn(C_2H_5)_4$), respectively.

2.3.2 Physical vapor method

Molecular beam epitaxy (MBE) is a physical vapor deposition method (PVD) to grow thin film material. MBE needs to work with high purity source material at ultrahigh vacuum conditions. It is different from the MOCVD; there is no carrier gas required. Thereby, the film grown by MBE is of very high quality; at the same time, the dopant concentration can be highly operated in a large range. In the MBE process, a pure Ga source is essential, which is evaporated from an effusion cell, while O is provided by O_2/ O_3 or from the RF-plasma. Same as MOCVD, MBE is applied for the growth of β-Ga_2O_3 both heteroepitaxially and homoepitaxially. Vogt et al. (2015, 2016a, 2016b), and Tsai et al. (2010) found that the desorption of gallium suboxide (Ga_2O) is a key factor that affects the growth rate of β-Ga_2O_3. Vogt et al. (2016b) pointed out that higher growth temperature caused a lower growth rate but higher quality. Besides the growth temperature, the Ga and O fluxes or beam equivalent pressure also affect the growth of β-Ga_2O_3. The commonly used conditions by MBE are as follows: 700-800 ℃ is the most used growth temperature, Ga/O flux is close to the stoichiometric ratio, 1-3 h growth time is always used (Oshima et al., 2017; Sasaki et al., 2013; Sasaki et al., 2012). For the homoepitaxial substrate, the orientation of the